Progress on Kinetic MHD Algorithms

Scott Parker, Jianhua Cheng, Yang Chen
University of Colorado, Boulder

Outline

- Status of Milestones
- Resulting publications
- Core ion damping of TAE
- Model equations
- 2nd order implicit method
- Tearing mode benchmark
- Including GK electrons

CEMM funding at Univ. of Colorado is $50,000 per year and supports one grad student (Jianhua Cheng)

CEMM Milestones

"Verify ... against linear kinetic theory of Alfven, whistler and ion Landau damping of acoustic waves." -- Done!

"Test enery conservation." -- Done!

"Compare current closure and pressure closure models for linear and nonlinear simulations." -- Nonlinear g-mode simulations done with pressure closure model only. Linear comparisons are done. PoP paper published on this comparison.

"Study ion kinetic effects on the nonlinear evolution of magnetic island." -- Progress to date, simulation of tearing instability and island formation. Expect nonlinear results very shortly from Jianhua Cheng, Univ. of Colorado.

"Comparison with nonlocal parallel closures." -- not applicable

CEMM publications the past two years

"Low-noise particle algorithms for extended MHD closure,"
D. Barnes, J. Cheng, S. Parker, *Phys. Plasmas* **15** 055702 (2008)

"Particle-in-cell simulation with Vlasov ions and drift kinetic electrons,"
Y. Chen, S. Parker, *Phys. Plasmas* **16** 052305 (2009)

"Gyrokinetic delta-f particle simulation of the TAE,"
J. Lang, Y. Chen, S. Parker, G. Fu, *Phys. Plasmas* **16** 052305 (2009)

Expect current/future work (Jianhua Cheng's Ph.D. thesis) will result in two additional publications. One on the second order implicit algorithm and one on reconnection with fully kinetic ions.

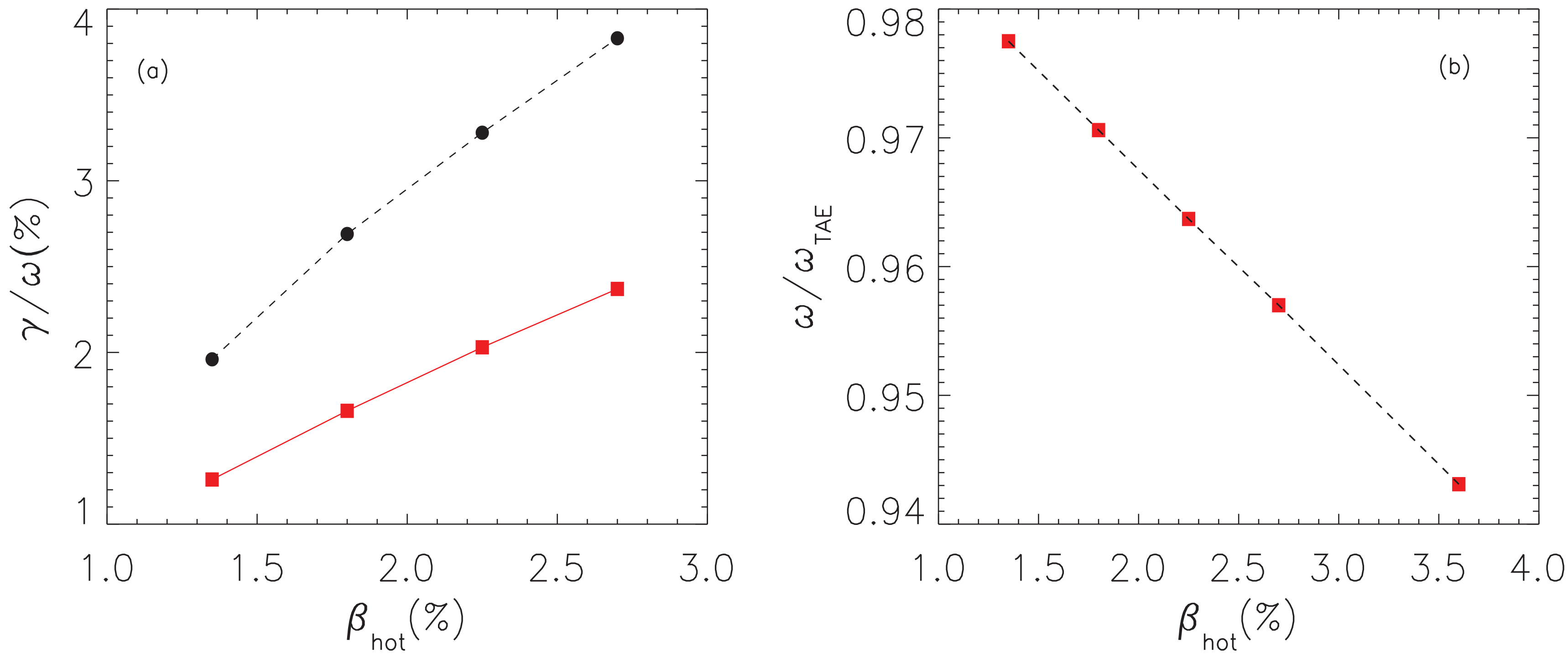

FIG. 12. (Color online) (a) The mode growth vs the energetic particle pressure. The black circles indicate the growth rate without the energetic particle FLR effect, and the red squares indicate the growth rate with the energetic particle FLR effect. (b) The mode frequency vs energetic particle pressure. This is from reduced model simulations.

The damping rate is extremely sensitive to the value of h_m so we should be very careful in estimating the mode frequency. We can estimate the continuum boundary ω_L and ω_U through the analytical formula [through Eq. (17)] or the eigenmode solutions mentioned in Sec. III A. These two results agree pretty well (within 1%) on the lower continuum between the damping rate and the thermal ion gyroradius is obtained, as shown in Fig. 14. This result shows reasonable agreement between simulations and theory. In analytical calculation, series expansion based on small thermal ion gyroradius is implied in the derivation of the gyrokinetic operator, where up to the fourth-order of $k_\perp \rho_i$ is retained, whereas

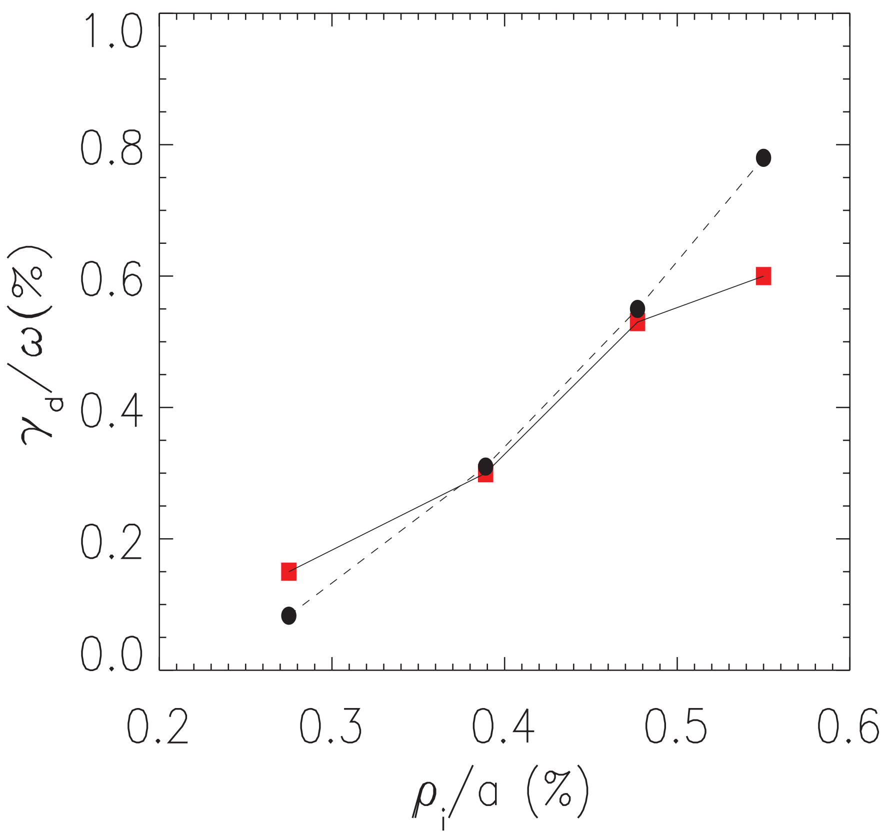

FIG. 14. (Color online) Comparison between theoretical calculation and simulations for the kinetic damping rate at different thermal ion gyroradii. The dashed line is from theory and the solid line is from simulation.

ing effect of energetic particles is investigated together with kinetic thermal ions, where kinetic damping effect from the background plasmas is observed. Particularly, we study the kinetic radiative damping using the fully gyrokinetic operator and compare it with analytical theory. As future work, it becomes feasible for GEM to study the Alfvénic mode excitation by the ion temperature gradient and the interaction between turbulence and TAEs with fully gyrokinetic thermal ions.

ACKNOWLEDGMENTS

We thank Dr. Nikolai Gorelenkov and Dr. T. S. Hahm for helpful discussions.

This work was supported by the Department of Energy's Scientific Discovery through Advanced Computing Program, "Center for Extended Magnetohydrodynamic Modeling," and by the U.S. Department of Energy under Grant No. DE-AC02-09-CH11466.

The Lorentz ion/Drift kinetic electron model

Lorentz ions:

$$\frac{d\mathbf{v}_i}{dt} = \frac{q}{m_i}(\mathbf{E} + \mathbf{v}_i \times \mathbf{B}), \qquad \frac{d\mathbf{x}_i}{dt} = \mathbf{v}_i$$

Drift kinetic electrons: $\varepsilon = \frac{1}{2} m_e v^2$

$$\frac{d\mathbf{x}}{dt} = \mathbf{v}_G \equiv v_\parallel \left(\mathbf{b} + \frac{\delta \mathbf{B}_\perp}{B_0} \right) + \mathbf{v}_D + \mathbf{v}_E$$

$$\frac{d\varepsilon}{dt} = -e\mathbf{v}_G \cdot \mathbf{E} + \mu \frac{\partial B}{\partial t}, \qquad \frac{d\mu}{dt} = 0$$

Ampere's equation

$$\nabla \times \mathbf{B} = \mu_0 (\mathbf{J}_i - e n_e (\mathbf{V}_{\mathrm{e}\perp} + u_{\parallel \mathrm{e}} \mathbf{b}))$$

$$\mathbf{V}_{\mathrm{e}\perp} = \frac{1}{B} \mathbf{E} \times \mathbf{b} - \frac{1}{enB} \mathbf{b} \times \nabla P_{\perp \mathrm{e}}$$

$$\mathbf{J}_i = \int f_i \mathbf{v} \, d\mathbf{v}, \qquad u_{\parallel \mathrm{e}} = \int f_e \, v_\parallel \, d\mathbf{v}, \qquad P_{\perp \mathrm{e}} = \int f_e \frac{1}{2} m_e v^2 \, d\mathbf{v}$$

Faraday's equation,

$$\frac{\partial \mathbf{B}}{\partial t} = -\nabla \times \mathbf{E}$$

Yang Chen, Scott E. Parker, Phys. Plasmas **16**, 052305 (2009).

Lorentz ion and fluid electron model

- Lorentz force ions:

$$\frac{d\boldsymbol{v}_i}{dt} = \frac{q}{m_i}(\boldsymbol{E} + \boldsymbol{v}_i \times \boldsymbol{B}), \qquad \frac{d\boldsymbol{x}_i}{dt} = \boldsymbol{v}_i$$

- Isothermal fluid electrons as a simple test:

$$\delta p_e = \gamma \delta n_e T_e = \gamma \delta n_i T_e.$$

Eventually we will add gyrokinetic electrons.

- Ampere's law:

$$\nabla \times \delta \boldsymbol{B} = \mu_0 e \left(n \boldsymbol{u_i} - n \boldsymbol{u_e} \right)$$

- Faraday's law

$$\nabla \times \boldsymbol{E} = -\frac{\partial\, \delta \boldsymbol{B}}{\partial t}.$$

Ohm's law

- Starting from the electron momentum equation:

$$\boldsymbol{E} = -\boldsymbol{u_i} \times \boldsymbol{B_0} + \frac{1}{\mu_0 en}(\bigtriangledown \times \delta\boldsymbol{B}) \times \boldsymbol{B_0} + \frac{\eta}{\mu_0} \bigtriangledown \times \delta\boldsymbol{B} - \frac{\nabla p_e}{en} - \frac{m_e}{en}\frac{\partial(n\boldsymbol{u_e})}{\partial t}.$$

- With Ampere's law and ion momentum equation

$$\bigtriangledown \times \delta\boldsymbol{B} = \mu_0 e\left(n\boldsymbol{u_i} - n\boldsymbol{u_e}\right)$$

$$\frac{\partial(n\boldsymbol{u_i})}{\partial t} = \frac{en}{m_i}(\boldsymbol{E} + \boldsymbol{u_i} \times \boldsymbol{B_0}) - \frac{1}{m_i} \bigtriangledown p_i.$$

- And neglect terms with m_e/M_i, we obtain Ohm's law

$$\boldsymbol{E} + \frac{c^2}{w_{pe}^2} \bigtriangledown \times(\bigtriangledown \times \boldsymbol{E}) = -\frac{\boldsymbol{J_i}}{en} \times \boldsymbol{B_0} + \frac{1}{\mu_0 en}(\bigtriangledown \times \delta\boldsymbol{B}) \times \boldsymbol{B_0}$$
$$+ \frac{\eta}{\mu_0} \bigtriangledown \times\delta\boldsymbol{B} - \frac{\gamma T_e \nabla n_i}{en}.$$

Implicit δf algorithm

- δf method for ions:

$$\frac{d}{dt}f_{i1} = -\frac{q}{m_i}(\boldsymbol{E} + \boldsymbol{v} \times \delta \boldsymbol{B}_1) \cdot \frac{\partial}{\partial \boldsymbol{v}} f_{i0}.$$

$$\frac{d}{dt}\omega_i = -\frac{q}{T_i}\boldsymbol{E} \cdot \boldsymbol{v}.$$

where the second equation comes from Maxwellian distribution.

- For ρ_i scale instabilities $k_\perp \rho_i \sim 1, \beta \sim 0.01$, the compressional wave frequency $\frac{\omega}{\Omega_i} \geq 10$, therefore $\Omega_i \Delta t \ll 0.01$ is needed. But in certain cases (e.g. NSTX), $\Omega_i \Delta t \sim 0.1$, which makes implicit method indispensable.

- A first-order scheme has been developed. Here we provide a second-order scheme with an improved field solver.

Yang Chen, Scott E. Parker, Phys. Plasmas **16**, 052305 (2009)

Second order implicit scheme

- Particle push

$$\frac{\boldsymbol{x}^{n+1}-\boldsymbol{x}^n}{\Delta t} = (1-\theta)\ \boldsymbol{v}^n + \theta\ \boldsymbol{v}^{n+1},$$

$$\frac{\boldsymbol{v}^{n+1}-\boldsymbol{v}^n}{\Delta t} = \frac{q}{m}\Big((1-\theta)\ (\boldsymbol{E}^n + \boldsymbol{v}^n \times \boldsymbol{B}_0) + \theta\ (\boldsymbol{E}^{n+1} + \boldsymbol{v}^{n+1} \times \boldsymbol{B}_0)\Big),$$

$$\frac{\omega^{n+1}-\omega^n}{\Delta t} = \frac{q}{T_{i0}}\Big((1-\theta)\ (\boldsymbol{E}^n \cdot \boldsymbol{v}^n) + \theta\ (\boldsymbol{E}^{n+1} \cdot \boldsymbol{v}^{n+1})\Big).$$

- Faraday's law

$$\frac{\delta\boldsymbol{B}^{n+1}-\delta\boldsymbol{B}^n}{\Delta t} = -[(1-\theta)\ \nabla \times \boldsymbol{E}^n + \theta\ \nabla \times \boldsymbol{E}^{n+1}].$$

- Ohm's law:

$$\boldsymbol{E}^{n+1} + \alpha\ \nabla \times \nabla \times \boldsymbol{E}^{n+1} + \theta\,\frac{\Delta t}{\beta_e}\left(\nabla \times \nabla \times \boldsymbol{E}^{n+1}\right) \times \boldsymbol{B}_0$$

$$= -\gamma \nabla n_i - \boldsymbol{J}^\star \times \boldsymbol{B}_0 + \frac{1}{\beta_e}\ (\nabla \times \delta\boldsymbol{B}^n) \times \boldsymbol{B}_0 + \frac{\eta}{\beta_e}\ \nabla \times \delta\boldsymbol{B}^n$$

$$-(1-\theta)\,\frac{\Delta t}{\beta_e}(\nabla \times \nabla \times \boldsymbol{E}^n) \times \boldsymbol{B}_0 - (1-\theta)\,\frac{\eta\Delta t}{\beta_e}\ \nabla \times \nabla \times \boldsymbol{E}^n.$$

$\alpha = \frac{m_e}{m_i}\frac{1}{\beta_e} + \theta\eta\Delta t$

Ion current

- First half push cycle

$$
\begin{aligned}
\boldsymbol{v}^\star &= \boldsymbol{v}^n + (1-\theta)\Delta t\,\frac{q}{m}\left(\boldsymbol{E}^n + \boldsymbol{v}^n \times \boldsymbol{B}_0\right),\\
\boldsymbol{x}^\star &= \boldsymbol{x}^n + (1-\theta)\Delta t\,\boldsymbol{v}^n,\\
\omega^\star &= \omega^n + (1-\theta)\Delta t\,\frac{q}{T_{i0}}\left(\boldsymbol{E}^n \cdot \boldsymbol{v}^n\right).
\end{aligned}
$$

- Dependence of $\boldsymbol{J}_i^{n+1}$ on $\boldsymbol{E}_1^{n+1}$

$$
\begin{aligned}
\boldsymbol{J}_i^{n+1} &= \boldsymbol{J}_i^\star + \theta\ \Delta t \frac{V}{N}\sum_j \frac{1}{\Delta V}\frac{q}{T_i}\boldsymbol{v}_j \boldsymbol{E}^{n+1}(\boldsymbol{x}_j^{n+1}) \cdot \boldsymbol{v}_j S(\boldsymbol{x} - \boldsymbol{x}_j^{n+1})\\
&\simeq \boldsymbol{J}_i^\star + \theta\ \Delta t\,\frac{q^2}{m}\,\boldsymbol{E}^{n+1} \equiv \boldsymbol{J}_i'.
\end{aligned}
$$

  where the second equation follows as the marker distribution is Maxwellian.

- In the following simulation, we find that replacing $\boldsymbol{J}_i^{n+1}$ with $\boldsymbol{J}_i'$ does not lead to observable difference. For accuracy issues, we iterate on the differences between $\boldsymbol{J}_i^{n+1}$ and $\boldsymbol{J}_i'$ while solving Ohm's law to obtain $\boldsymbol{E}^{n+1}$.

3-D Shearless Slab Alfven waves

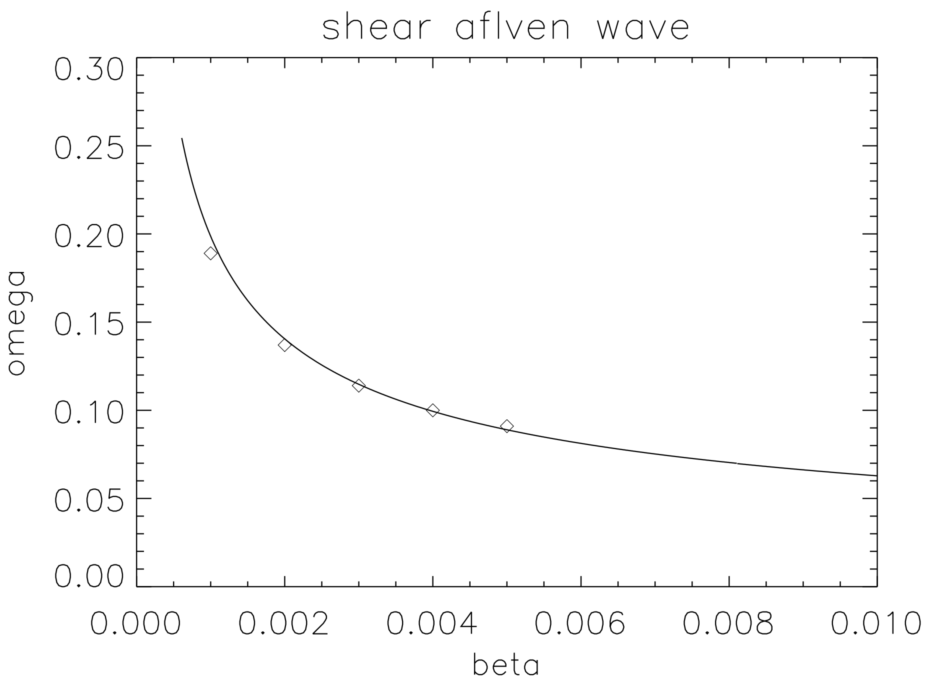

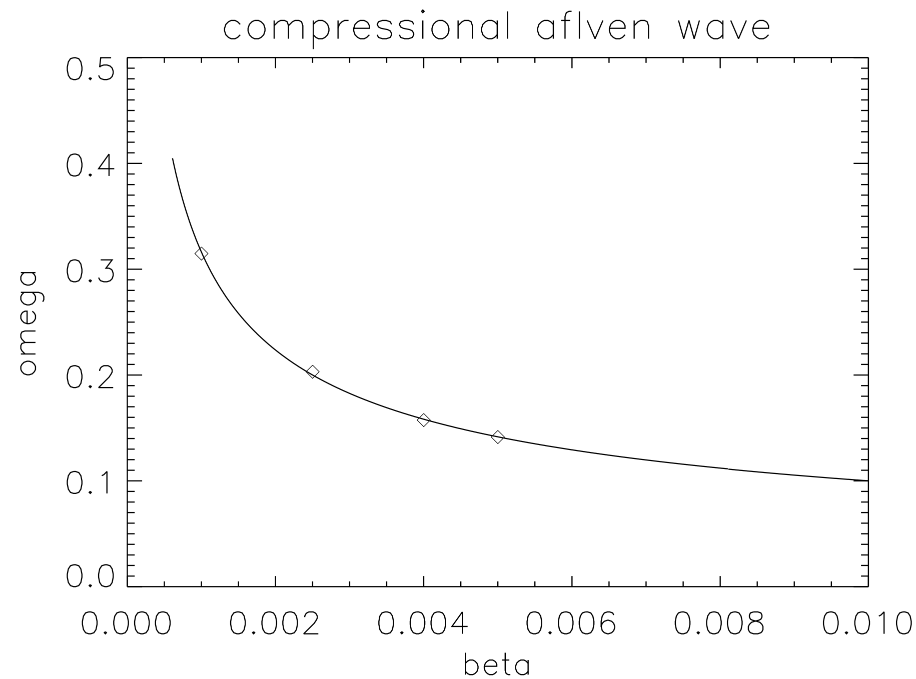

$2 \times 32 \times 32$ grids, 131072 particles.

For shear Alfven wave, $k_\perp = 0$, $k_\parallel \rho_i = 0.00628$, initialize with $\delta \boldsymbol{B}_\perp$.

For compressional Alfven wave, $k_\parallel = 0$, $k_\perp \rho_i = 0.01$, initialize with $\delta \boldsymbol{B}_\parallel$.

These simulations are done in a tilted B_0 field.

Ion acoustic wave

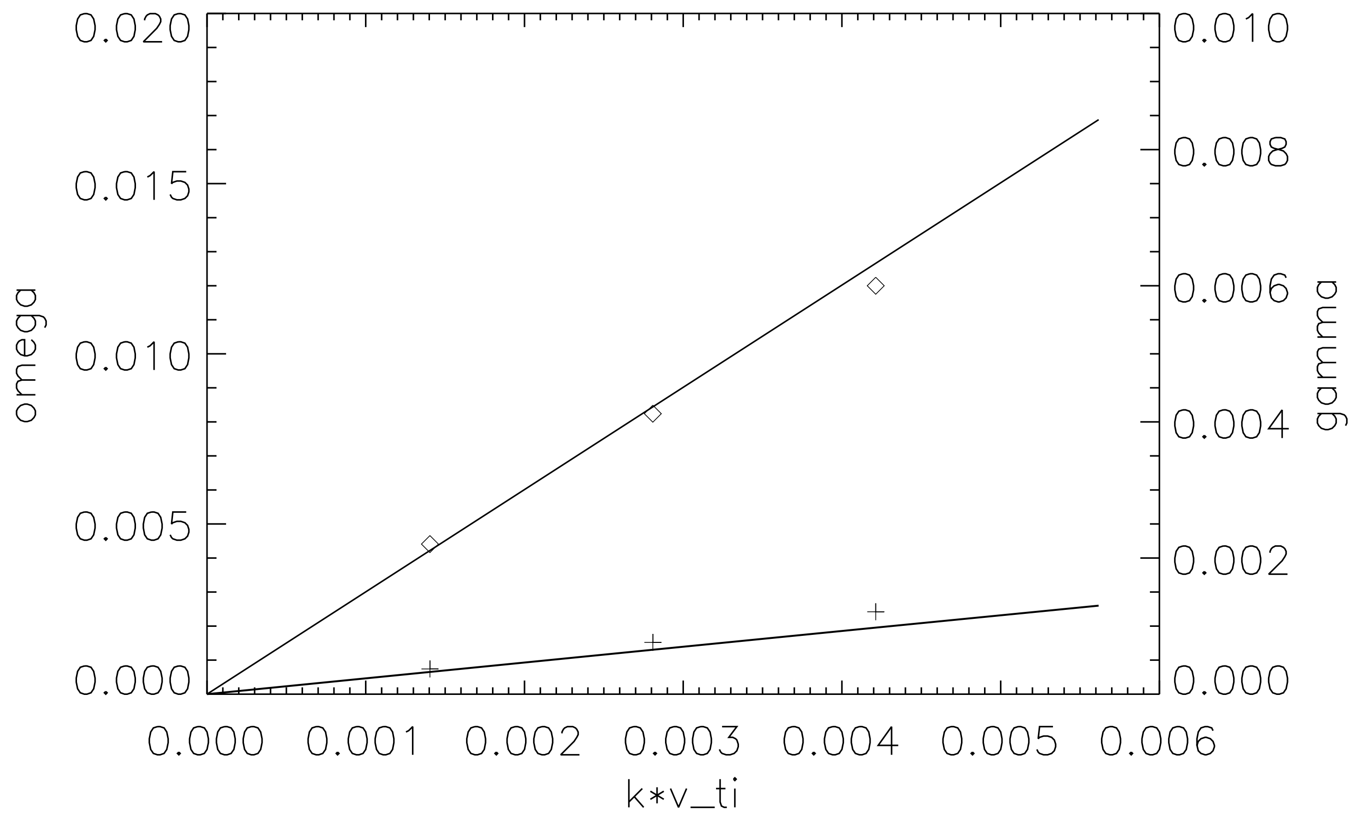

$2 \times 32 \times 32$ grids, 131072 particles. $k_\perp = 0$.

Whistler wave

- By neglecting ion current and electron inertia, the Ohm's law yields

$$\boldsymbol{E} = \frac{1}{\beta_e} (\nabla \times \delta \boldsymbol{B}) \times \boldsymbol{B}_0.$$

- Numerical form

$$\boldsymbol{E}^{n+1} + \theta \, \frac{\Delta t}{\beta_e} \left(\nabla \times \nabla \times \boldsymbol{E}^{n+1}\right) \times \boldsymbol{B}_0$$
$$= \frac{1}{\beta_e} \, (\nabla \times \delta \boldsymbol{B}^n) \times \boldsymbol{B}_0 - (1-\theta) \, \left(\frac{\Delta t}{\beta_e} \nabla \times \nabla \times \boldsymbol{E}^n\right) \times \boldsymbol{B}_0$$

- The numerical dispersion relation from a Von Neumann stability analysis

$$\tan(\omega_r \Delta t) = \frac{\frac{k^2}{\beta}\Delta t}{1 - (\frac{k^2}{\beta}\Delta t)^2 \, \theta(1-\theta)}$$
$$\omega_i \Delta t = -\frac{1}{2} \ln \left(\frac{\left(1 - (\frac{k^2}{\beta}\Delta t)^2 \, \theta(1-\theta)\right)^2 + (\frac{k^2}{\beta}\Delta t)^2}{\left(1 + (\frac{k^2}{\beta}\Delta t)^2 \, (1-\theta)^2\right)^2} \right)$$

Numerical dispersion relation

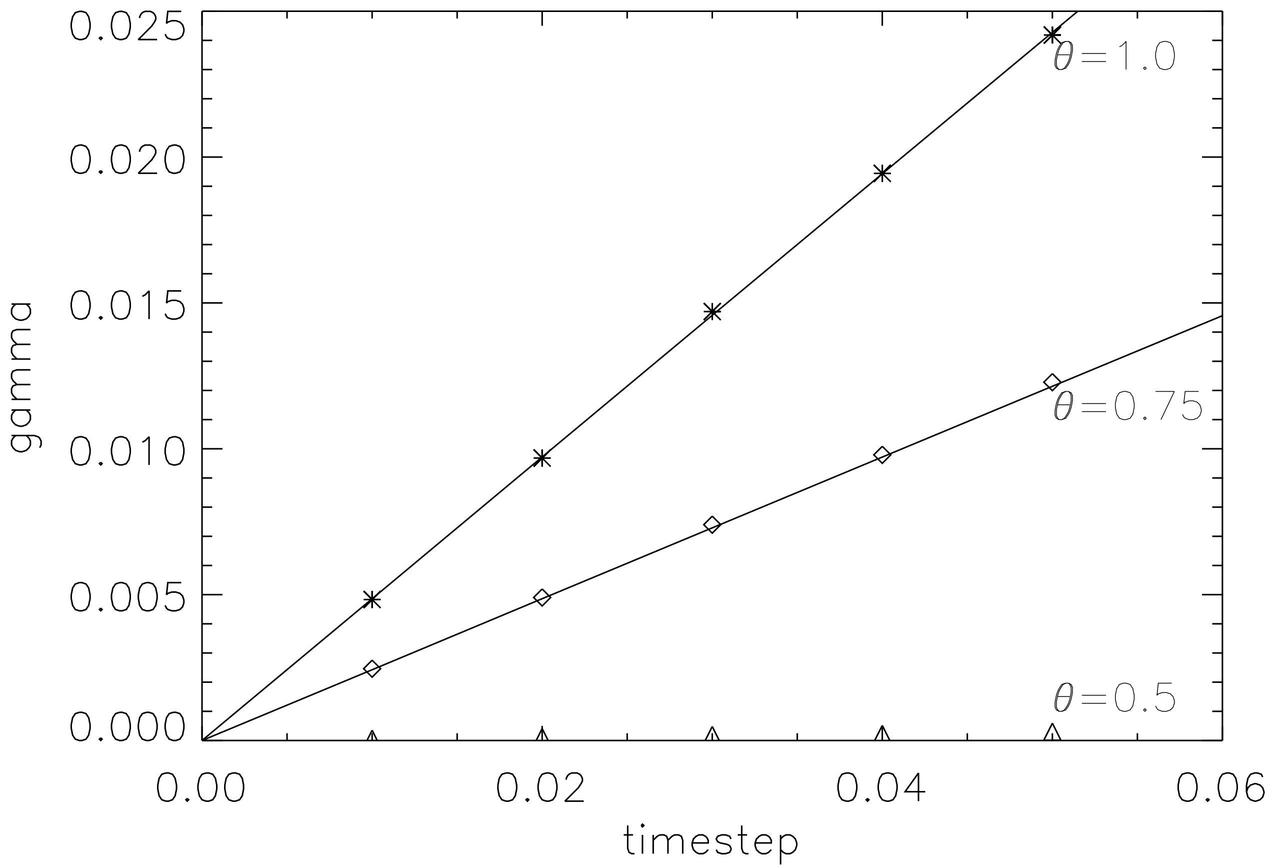

$16 \times 16 \times 32$ grids, 131072 particles, $k_\perp = 0$, $k_\parallel = 0.0628$, $\beta = 0.004$.

Harris sheet equilibrium

- Zero-order $\boldsymbol{B}$

$$\boldsymbol{B}(\boldsymbol{x}) = B_{y0} \tanh(\frac{x}{L})\ \hat{\boldsymbol{y}} + B_G\ \hat{\boldsymbol{z}}$$

- The equilibrium distribution function is

$$f_{0s} = n_h \ \mathrm{sech}^{\,2}(\frac{x}{L}) \left(\frac{2\pi T_s}{m_s}\right)^{-\frac{3}{2}} \exp\left[-\frac{m(v_x^2 + v_y^2 + (v_z - v_{ds})^2)}{2T_s}\right]$$

$$+n_b \ \left(\frac{2\pi T_s}{m_s}\right)^{-\frac{3}{2}} \exp\left(-\frac{mv^2}{2T_s}\right)$$

- Load particles as Maxwellian

$$g_s = n_0 \left(\frac{2\pi T_s}{m_s}\right)^{-\frac{3}{2}} \ \exp\left(-\frac{m_s \boldsymbol{v}^2}{2T_s}\right)$$

- Weight equation

$$\frac{d\omega_i}{dt} = \frac{q_s}{T_s} \ \left(\boldsymbol{E} \cdot \boldsymbol{v}(\frac{f_h}{g_s} + \frac{n_b}{n_0}) - \boldsymbol{v}_d \cdot (\boldsymbol{E} + \boldsymbol{v} \times \delta\boldsymbol{B})\ \frac{f_h}{g_s}\right)$$

$$\frac{f_h}{g_s} = \frac{n_h}{n_0} \ \mathrm{sech}\,(\frac{x}{L})^2 \ \exp\left(\frac{m_s}{2T_s}\ (2\boldsymbol{v}_d \cdot \boldsymbol{v} - \boldsymbol{v}_d^2)\right).$$

Boundary conditions

- Since the zero order magnetic field $\boldsymbol{B}_{y0}$ is sheared in x-direction, perfect conducting wall boundary condition is employed. While periodic boundary condition is still used in y and z direction.

$$\boldsymbol{E}_{y,z}|_{x=\pm l_x/2} = 0$$
$$\delta\boldsymbol{B}_x|_{x=\pm l_x/2} = 0$$

- Numerically, the boundary condition for $\boldsymbol{E}$ can be treated as

$$\frac{\boldsymbol{E}_{y,z}^{-1} + \boldsymbol{E}_{y,z}^{1}}{2} = 0$$
$$\frac{\boldsymbol{E}_{x}^{-1} + \boldsymbol{E}_{x}^{1}}{2} = \boldsymbol{E}_x^0$$

  at $x = -l_x/2$ and similarly at $x = l_x/2$.

- Boundary condition for $\delta\boldsymbol{B}$ is considered in Faraday's equation.

- All the previous simulation results of cold plasma waves are recovered within this new boundary condtion.

Resistive Tearing mode

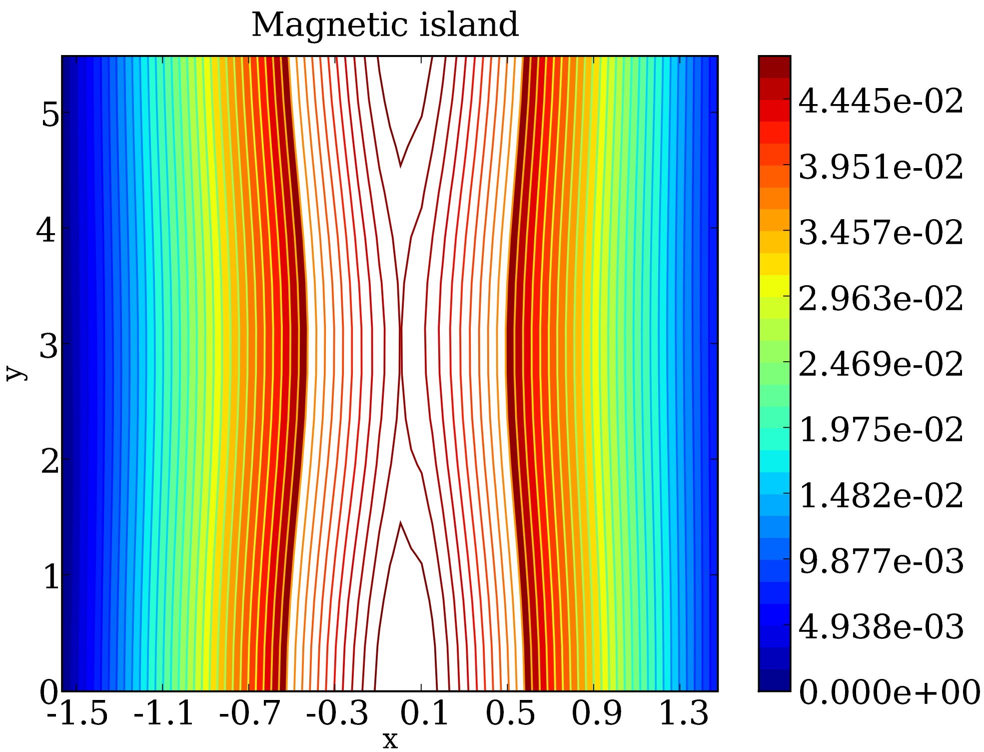

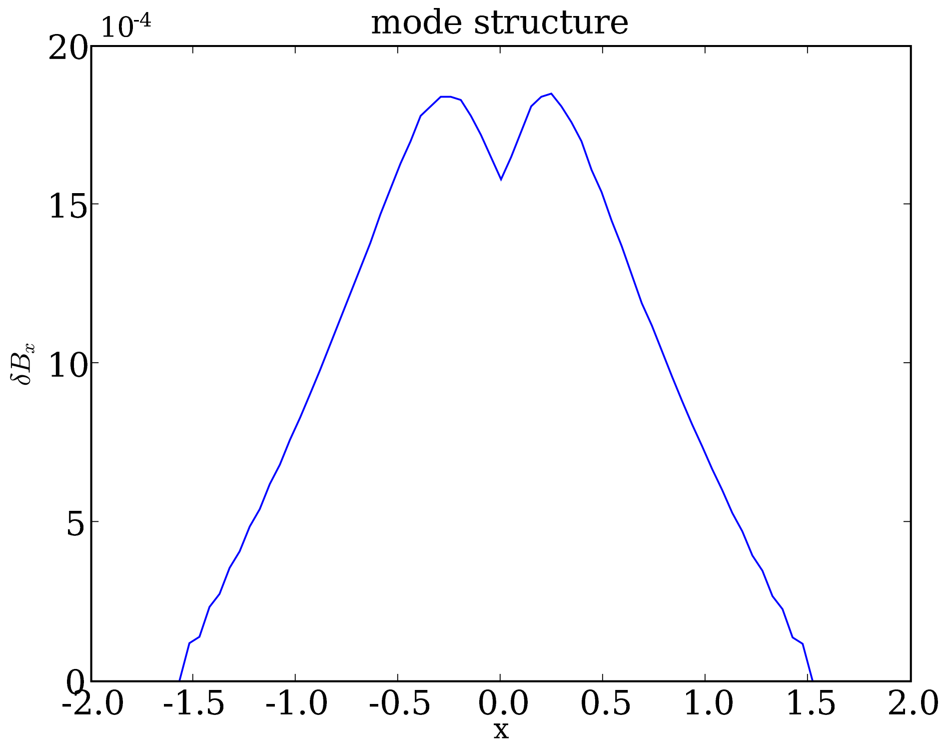

$64 \times 16 \times 16$ grids, 131072 particles. $k_y = 1.0, L = 0.25, \beta = 0.2,$

$\eta = 0.0005, \boldsymbol{B}_G = 1, T_i/T_e = 1, l_x = 3.14, l_y = 6.28$

Tearing mode growth rate vs. resistivity

- Linear Tearing mode theory shows that the growth rate is (scaled)

$$\gamma = 0.55\ (\frac{\Delta'}{\beta})^{4/5}\ \eta^{3/5}\ (k\ B'_{y0})^{2/5}.$$

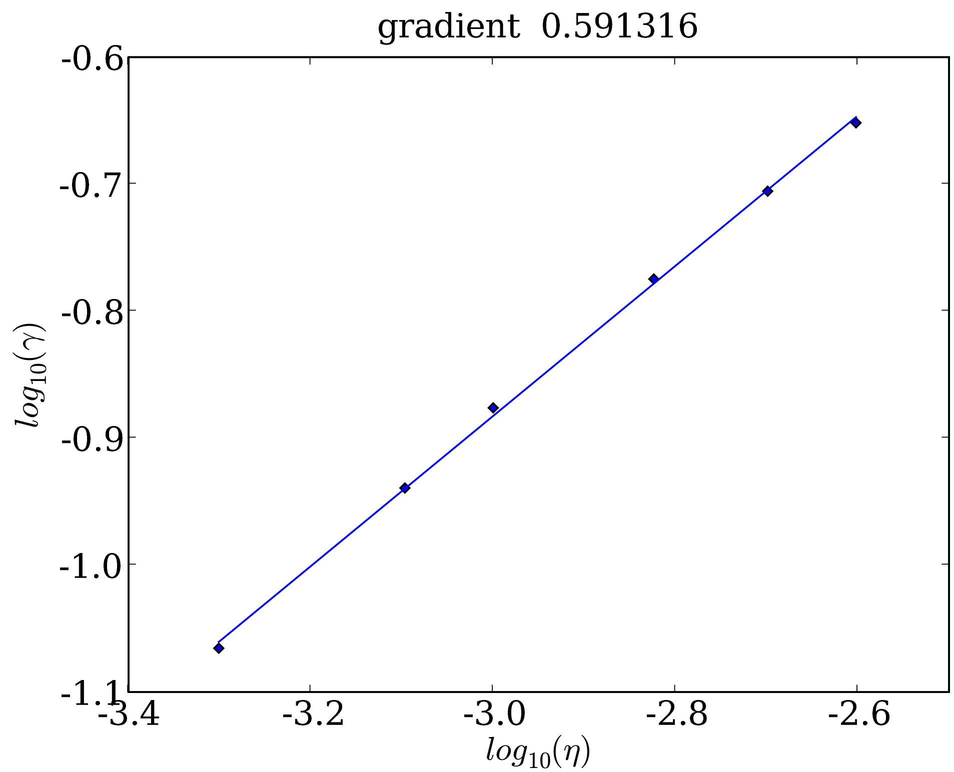

- The gradient is 0.59, which is pretty close to the expected 0.6.

Including gyrokinetic electrons

- Gyrokinetic equations are usually derived in terms of $\mathbf{A}$ and ϕ, to make explicit the ordering

$$\frac{\partial \mathbf{A}}{\partial t} \sim \epsilon_\delta \nabla_\perp \phi$$

- The Frieman-Chen gyrokinetic equation, assuming isotropy $(\partial F_0/\partial \mu = 0)$,

$$\hat{L}_g \delta H_0 \equiv \left(\frac{\partial}{\partial t} + v_\parallel \mathbf{b} \cdot \nabla + \mathbf{v}_D \cdot \nabla \right) \delta H_0 = -\frac{q}{m}(S_L + \langle R_{\mathrm{NL}} \rangle),$$

where δH_0 is related to the perturbed distribution δF through $\delta F = \frac{q}{m}\phi \frac{\partial F_0}{\partial \epsilon} + \delta H_0$

$$S_L = \frac{\partial}{\partial t} \langle \phi - \mathbf{v} \cdot \mathbf{A} \rangle \frac{\partial F_0}{\partial \epsilon} - \nabla \langle \phi - \mathbf{v} \cdot \mathbf{A} \rangle \times \frac{\mathbf{b}}{\Omega} \cdot \nabla F_0,$$

$$\langle R_{\mathrm{NL}} \rangle = -\nabla \langle \phi - \mathbf{v} \cdot \mathbf{A} \rangle \times \frac{\mathbf{b}}{\Omega} \cdot \nabla \delta H_0.$$

- Define $\delta f = \frac{q}{m} \langle \phi \rangle \frac{\partial F_0}{\partial \epsilon} + \delta H_0$. The gyrokinetic equation for δf is, written in terms of $\mathbf{E}_1$ and $\mathbf{B}_1$

$$\frac{D}{Dt}\delta f = -\left(\frac{1}{B_0} \langle \mathbf{E}_1 \rangle \times \mathbf{b} + v_\parallel \frac{\langle \mathbf{B}_{1\perp} \rangle}{B_0} \right) \cdot \nabla F_0 + \frac{1}{m} \dot{\epsilon} \frac{\partial F_0}{\partial \epsilon}$$

$$\frac{D}{Dt} = \hat{L}_g + \left(\frac{1}{B_0} \langle \mathbf{E}_1 \rangle \times \mathbf{b} + v_\parallel \frac{\langle \mathbf{B}_{1\perp} \rangle}{B_0} \right) \cdot \nabla, \qquad \dot{\epsilon} = q \left(v_\parallel \mathbf{b} + \mathbf{v}_D + v_\parallel \frac{\langle \mathbf{B}_{1\perp} \rangle}{B_0} \right) \cdot \langle \mathbf{E}_1 \rangle + q \langle \mathbf{v}_\perp \cdot \mathbf{E}_{1\perp} \rangle$$

- The perturbed electron diamagnetic flow comes from δf,

$$n_0 \mathbf{V}_D(\mathbf{x}) = \int (v_\parallel \mathbf{b} + \mathbf{v}_\perp(\mathbf{R}', \epsilon, \mu, \alpha))\delta f(\mathbf{R}', \epsilon, \mu)\delta(\mathbf{x} - \mathbf{R}' - \boldsymbol{\rho})\, J d\mathbf{R}'\, d\epsilon\, d\mu\, d\gamma$$

$n_0 \mathbf{V}_D$ is computed by depositing the particle current along the gyro-ring. In the drift-kinetic limit $\mathbf{V}_D$ reduces to the electron diamagnetic flow.

- The electron $\mathbf{E} \times \mathbf{B}$ flow comes from the first term in δF,

$$n_0 \mathbf{V}_E(\mathbf{x}) = \frac{\mathbf{q}}{\mathbf{m}} \int \mathbf{v} \left(\phi(\mathbf{x}) - \langle \phi \rangle (\mathbf{x} - \boldsymbol{\rho}, \epsilon, \mu)\right) \frac{\partial \mathbf{F_0}}{\partial \epsilon} \mathbf{J}\, \mathbf{d}\epsilon\, \mathbf{d}\mu\, \mathbf{d}\gamma$$

in eikonal form,

$$n_0 \mathbf{V}_E = n_0 \frac{h}{B_0} \delta \mathbf{E}_k \times \mathbf{b}$$

with $b = k_\perp^2 v_T^2 / \Omega^2$ and

$$h(b) = -\frac{1}{b^2} \int_0^\infty e^{-x^2/2b} J_0(b) J_0'(b) x^2\, dx$$

In the limit of small $k\rho \ll 1$ the factor $h(b)$ become unity, so that $n_0 \mathbf{V}_E$ become the total guiding center $\mathbf{E} \times \mathbf{b}$ flow.

Summary

Major progress the past two years, completion of milestones, 3 publications

Core ion damping of TAE

Lorentz ion, drift kinetic ion implicit algoritm

Second order implicit algorithm now working

Code produces all linear (kinetic) waves as expected from theory

Tearing mode simulation shows island growth and agrees with theory

(Published) Thought put into how to implement GK electrons

Future work (next 6 months or when we meet again)

Nonlinear simulation of reconnection --
nonlinear evolution of a island perturbation